Electronic Supporting Information

Carbon nanowalls: A new versatile graphene based interface for laser desorption/ionization-mass spectrometry detection of small compounds in real samples

I.S. Hosu[a], M. Sobaszek[b], M. Ficek[b], R. Bogdanowicz[b], H. Drobecq[c], L. Boussekey[d], A. Barras[a], O. Melnyk[c], R. Boukherroub[a] and Y. Coffinier [a]*

[a] *Univ. Lille, CNRS, Centrale Lille, ISEN, Univ. Valenciennes, UMR 8520 - IEMN, F-59000 Lille, France*
[b] *Faculty of Electronics, Telecommunication and Informatics, Gdansk University of Technology, 11/12 Narutowicza St. 80-233, Gdansk, Poland.*
[c] *Institut de Biologie de Lille (IBL, CNRS-UMR 8161), Université de Lille Nord de France, IFR142, 1 rue du Pr. Calmette, 59021 Lille, France.*
[d] *Laboratoire de Spectrochimie Infrarouge et Raman, CNRS UMR 8516, Cité Scientifique, Université Lille1, 59655 Villeneuve d'Ascq, France*
(*) Contact: email: yannick.coffinier@univ-lille1.fr

1. Instrumentation and surface characterization

1.1. X-ray photoelectron spectroscopy

For X-ray photoelectron spectroscopy (XPS) measurements (Type 5600, Physical Electronics Inc., Chanhassen, MN, USA), we used a monochromatic Al Kα X-ray source and an analyzer pass energy of 12 eV. The acceptance angle of the analyzer has been set to 14°, and the angle between the incident X-rays and the analyzer is 90°. The detection angle of the photoelectrons is 25°, as referenced to the sample surface. The intensities of the various XPS core levels (CLs) are measured as the peak area after standard background subtraction according to the Shirley procedure.

2. Experimental part

2.1. Growth of carbon boron-doped nanowalls (CNWs)

CNWs were synthesized in an MW PA CVD system (Seki Technotron AX5400S, Japan) on *p*-type Si wafers with (100) orientation. Substrates were cleaned by sonication in acetone and 2-propanol for 5 min in each solvent. Next, the substrates were seeded in nanodiamond suspension (crystallite size of 5–10 nm) for 60 min under sonication. Finally, the substrates were dried under a stream of nitrogen. Previously, we have shown that seeding procedure yields high seeding densities in the range up to 10^{10} cm^{-2}.[1,2] The substrate temperature was kept at 700°C during the deposition process. Excited plasma was ignited by microwave radiation (2.45 GHz). The microwave power was kept at 1300 W to achieve highly ionized plasma. The base pressure was about 10^{-6} Torr, while the process pressure was kept at 50 Torr. The source gas mixture of $H_2/CH_4/N_2$ at gas volume 300 sccm of total flow rate was applied. Moreover, the doping level of boron in the gas phase, expressed as [B]/[C] ratio, was kept at 1200 ppm using diborane (B_2H_6) as dopant precursor. The growth time was 6 h, producing surfaces with randomly vertically aligned nanowalls with the height of approx. 4 μm.

2.2. MS sample preparation

Solutions of saccharides were prepared in Milli-Q water or NaCl (10 mM) aqueous solutions. Peptides were prepared in ammonium citrate dibasic (1 mM) or ammonium phosphate monobasic $NH_4H_2PO_4$, (that also contained 0.1% TFA). The peptides solutions were prepared as recommended by the producer, but no organic matrix was added: 100 μL of water was added in standard tubes containing peptides. After vortexing, usually 1 μL of calibrant was mixed in 24 μL of the desired salt solution (citrate or phosphate). Unless otherwise stated, the peptides concentrations are presented in **Table S1** and the saccharides concentration is 5 nmol, in a total volume of 0.5 μL.

Table S1. Composition of calibration mixtures, protonated masses expected in MS and final concentrations of the prepared solutions (MIX 1 reflector mode, MIX 2 linear mode)

Compound	Abbreviated name	Charge (n)	$(M+nH)^{n+}$ Average	Final concentration for MS analysis (fmol/0.5 µL)	Signal/noise (S/N)		
					CNWs This work	BDDNWs [3a]	SiNWs [4b]
Calibration Mixture 1 (MIX 1)							
des-Arg1-Bradykinin	DAB	+1	905.05	25	465	1078	641
Angiotensin I	AI	+1	1,297.51	32.5	77	431	532
Glu1-Fibrinopeptide B	FPB	+1	1,571.61	32.5	71	55	100
Neurotensin	NT	+1	1,673.96	12.5	10	59	40
Calibration Mixture 2 (MIX 2)							
Angiotensin I	AI	+1	1,297.51	500	160	-	-
ACTH (clip 1–17)	ACTH1	+1	2,094.46	500	66	-	-
ACTH (clip 18–39)	ACTH18	+1	2,466.72	350	72	-	-
ACTH (clip 7–38)	ACTH7	+1	3,660.19	750	493	-	-
Insulin (bovine)	INS	+1	5,734.59	875	18	-	-
		+2	2,867.80	-	-	-	-

[a] 25 fmol/0.5 µL of DAB, AI and FPB and 5 fmol/0.5 µL of NT, ref[3]

[b] 25 fmol/0.5 µL of DAB, AI and FPB and 5 fmol/0.5 µL of NT, ref[4]

2.3. Functionalization of CNWs with OTS and surface patterning

In order to study the influence of the surface chemistry and to compare the MS performance for the as-synthesized CNWs with the oxidized CNWs (oxCNWs), several procedures were followed: for cleaning the surface of any remaining analyte, the sample was immersed in a piranha solution (H2O2:H2SO4=1:3) during 15 min. This process was repeated 2 times. The surface was activated 20 min under UV/ozone to create hydroxyl groups on the surface and after this treatment, the WCA was 13°. After rinsing abundantly with water and drying with a nitrogen flow, the surface was coated with OTS, using the following procedure: the CNWs surfaces were immersed into a 10−3 M solution of OTS in hexane for 6 h at room temperature, in a dried nitrogen-purged glovebox and the resulting surfaces were rinsed with CH2Cl2, isopropyl alcohol, and dried under a gentle stream of nitrogen. The WCA after OTS-modification was ~127°)4. This procedure is also presented in Scheme S1A. To create patterns that will concentrate the analyte in a specific hydrophilic surface area, we used UV lithography to locally remove the OTS. The steps are summarized in Scheme S1B. The first steps consist of spin-coating of the photoresist A4562 (using a speed of 3000 RPM, acceleration

2000, during 40s) and soft baking during 2.5 min at 110°C. For the UV exposure, an optical mask bearing patterns consisting of circles of 800 µm in diameter with an interspacing of 1800 µm was used. The exposure was done for 60 s and the gap distance was 100 µm. After the exposure, the surface was annealed 60 s at 110°C and then dipped in A351 developer during 15 s, and rinsed with water and dried under nitrogen flow. The patterns can be observed after this step. Oxygen plasma treatment was performed during 30 sec using RIE (reactive ion etching), with the following parameters: RF power 200W, pressure 100 mT and 30 sccm flow. This step is mandatory to remove the remaining resist inside the apertures and destroy the OTS layer. Then, the non-irradiated resist was removed by dipping the surface in acetone at 30°C during 20 min, rinsing with isopropanol and drying under nitrogen flow.

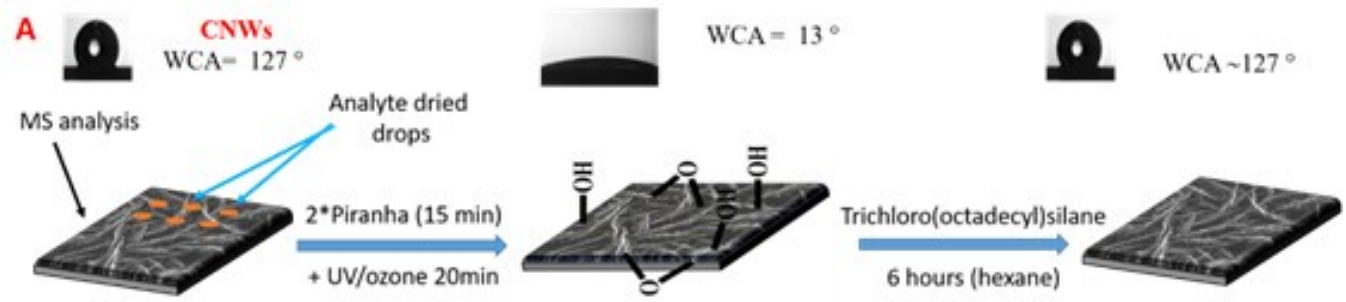

Scheme S1A. Surface cleaning and oxidation with piranha and UV/ozone, followed by OTS-modification.

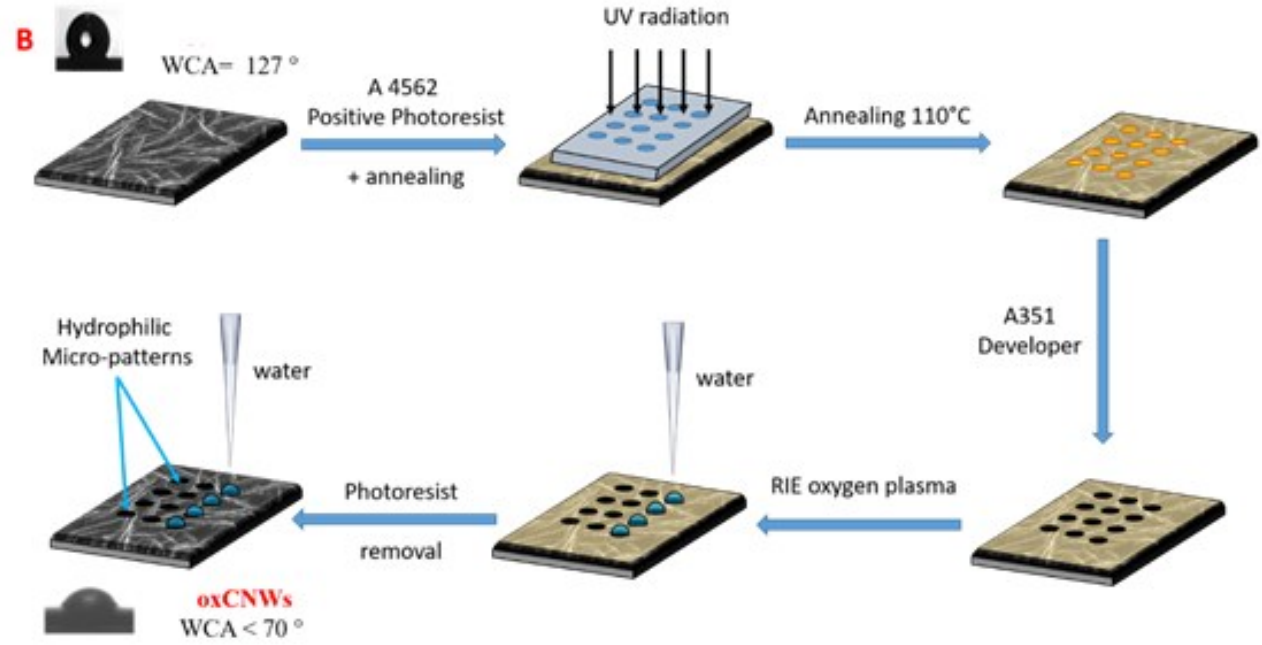

Scheme S1B. Hydrophilic micro-patterns designing procedure.

2.4. Surface characterizations

Diffuse reflectance measurements.

The diffuse reflectance absorption spectra (DRS) of the CNW samples were recorded on a UV–Vis-NIR spectroradiometric system (OL 750, Gooch & Housego, US) attached with an integrated sphere, and the spectra were recorded in the range of 350–1800 nm.

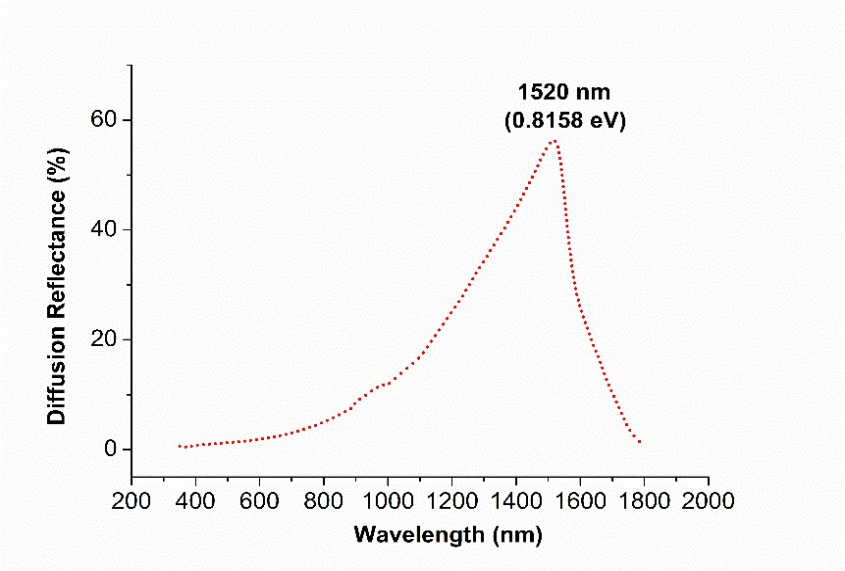

Fig. S1: Diffusion reflectance spectroscopy of CNWs.

Synthesis of benzylpyridinium compounds and internal energy calculation

Benzylpyridinium compounds were synthesized from the condensation of the corresponding para-substituted benzyl chloride (BzPy), with pyridine, using an excess of pyridine:benzylchloride (20:1 moles). The mixture was refluxed for 5 h at 60°C. After the reaction was completed, the mixture was cooled down at room temperature and benzylpyridinium was precipitated with diethyl ether. The excess of pyridine was removed under vacuum, at 80°C, and then dried at 60°C. No further purification was performed. All the benzylpyridinium compounds were named as follows, according to the element in the para position of the benzyl ring: BzPy (no substitute), CNBzPy (ciano group), ClBzPy (chloride group), FBzPy, (fluoride group) and NO_2BzPy (nitro group).

Benzylpyridinium compounds, called also “thermometer molecules” can be used to determine the deposited internal energies. For the calculation of the deposited internal energy, the approach that uses multiple benzylpyridinium’s critical energies was used.[5] The SY values were plotted versus critical energies (**Fig. S2**), and the values at 62% were fitted with a Boltzman function (**Fig. S3A**, R^2= 0.9998). The second derivative was applied to determine the internal energy distribution ρ(E), of the deposited internal energies (**Fig. S3B**).

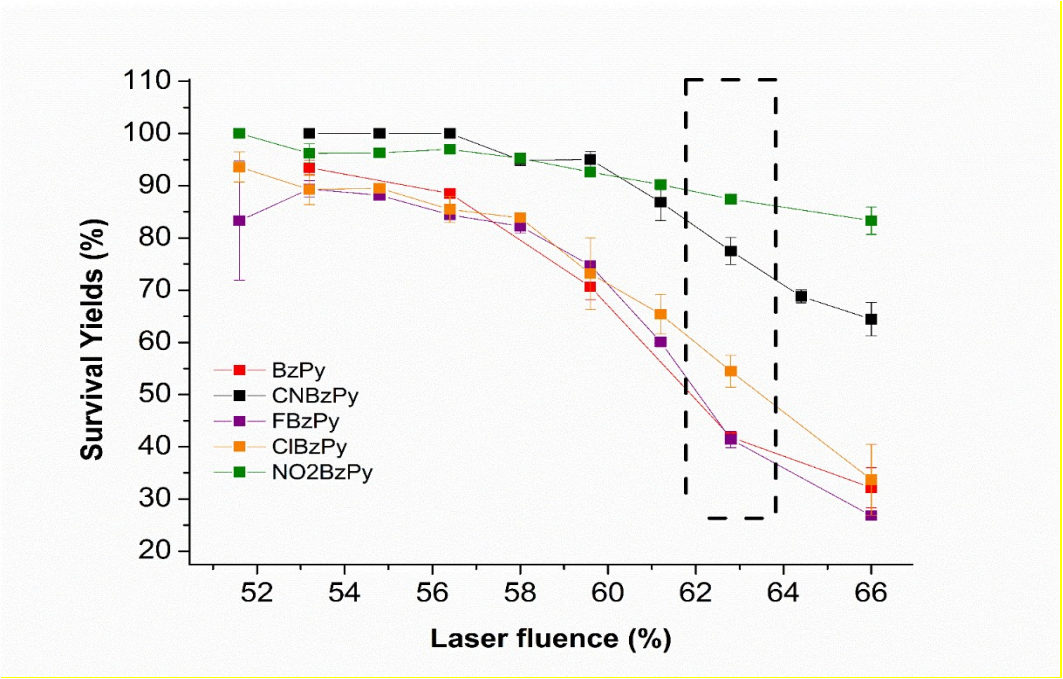

Fig. S2: Survival yields for 5 *p*-substituted benzylpyridinium ions (1 mM) as a function of laser fluence on CNWs.

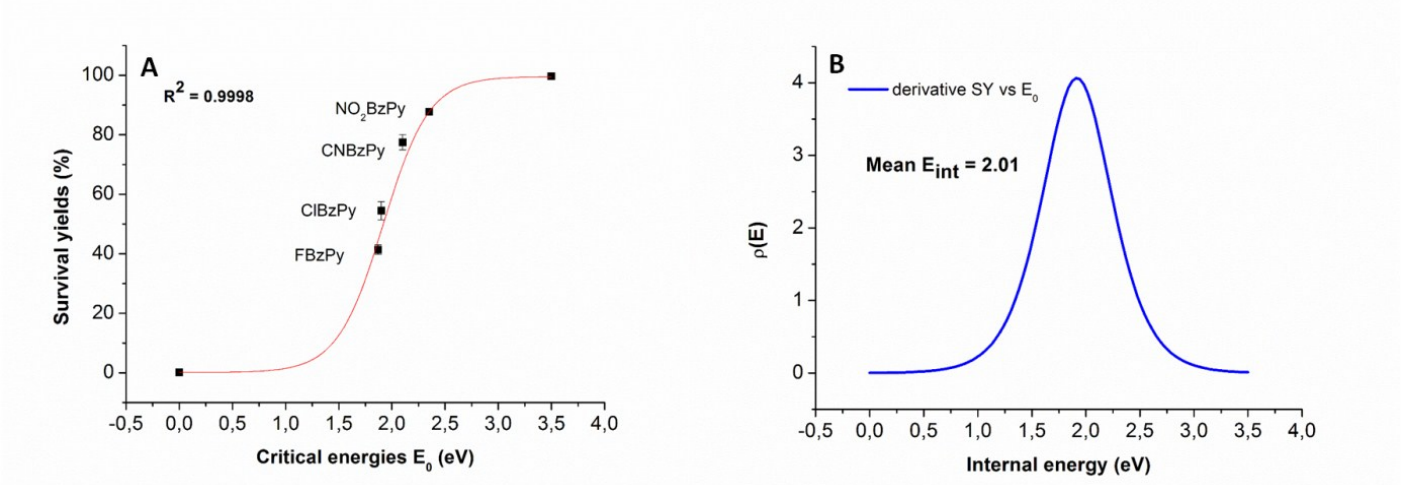

Fig. S3: Internal energy depositions for CNWs: (A) Survival yield values were plotted as a function of critical energy, E_o, at a laser fluence of 62% (3 measurements). (B) Derivatives of the sigmoidal curves produced the internal energy distributions ρ(E).

X-ray photoelectron spectroscopy (XPS)

Fig. S4 presents the XPS results of the C_{1s} and O_{1s} of the CNWS and the oxCNWs. For CNWs, the C_{1s} spectrum reveals that upon oxygen plasma during 30 s, the carbon atomic percentage decreases from 96.25 to 89.61 % (**Fig. S4A**), while the O_{1s} spectrum reveals that the atomic percentage of the oxygen increases from 2.98 to 9.25 % (**Fig. S4B**), meaning that oxidized carbon species are formed. The high resolution C_{1s} XPS spectrum of CNWs can be deconvoluted using CASA-XPS software into five peaks with binding energies at 281.9, 284.3, 285.8, 287.3 and 288.3 eV assigned to sp^2-hybridized carbon, C–H/C–C, C–O/O-C-O, C=O and O-C=O species, respectively (**Fig. S4C**). Similar

deconvolution was performed for the oxCNWs (**Fig. S4D**). Upon comparison, after oxygen plasma, the atomic percentage of the hydroxyl groups increased from 12.73 % to 26.23 % and carboxylic groups from 2.35% to 4.93%. As it can also be seen in the O_{1s} spectrum, the signal intensity decreases, in concordance with the above statement. As an overall argument, the C/O ratio decreases from 32.29 to 9.69, after the oxidation of CNWs by oxygen plasma. It has to be noticed that after piranha treatment, a C/O ratio value of 20.66 was obtained showing lower oxidation than after oxygen plasma treatment (see **Table S2**).The presence of boron was also assessed and we can see that no significant changes were observed (data not shown). The presence of fluorine can be attributed to some contamination during the synthesis of CNWs, in the MW PECVD chamber and the presence of nitrogen was accounted for acetone residues during the removal of the photoresist (as-synthesized CNWs did not shown any residual nitrogen).

Table S2. C/O ratios from XPS analyses from as-received CNWS and oxidized CNWs (Ox-CNWs) after piranha and oxygen plasma treatment.

XPS	Treatment	C/O
CNWs	As-received	32.29
Ox-CNWs	Piranha (H_2SO_4/H_2O_2 3:1), 15 min	20.66
Ox-CNWs	oxygen plasma 30 sec, 200 W, 100 mTorr	9.69

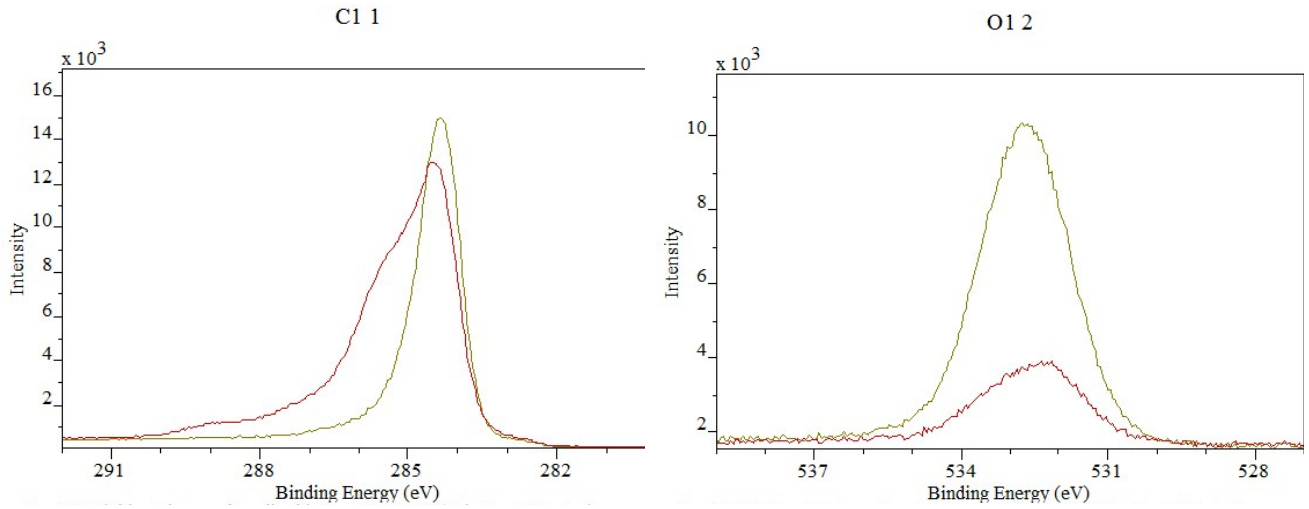

(A) **(B)**

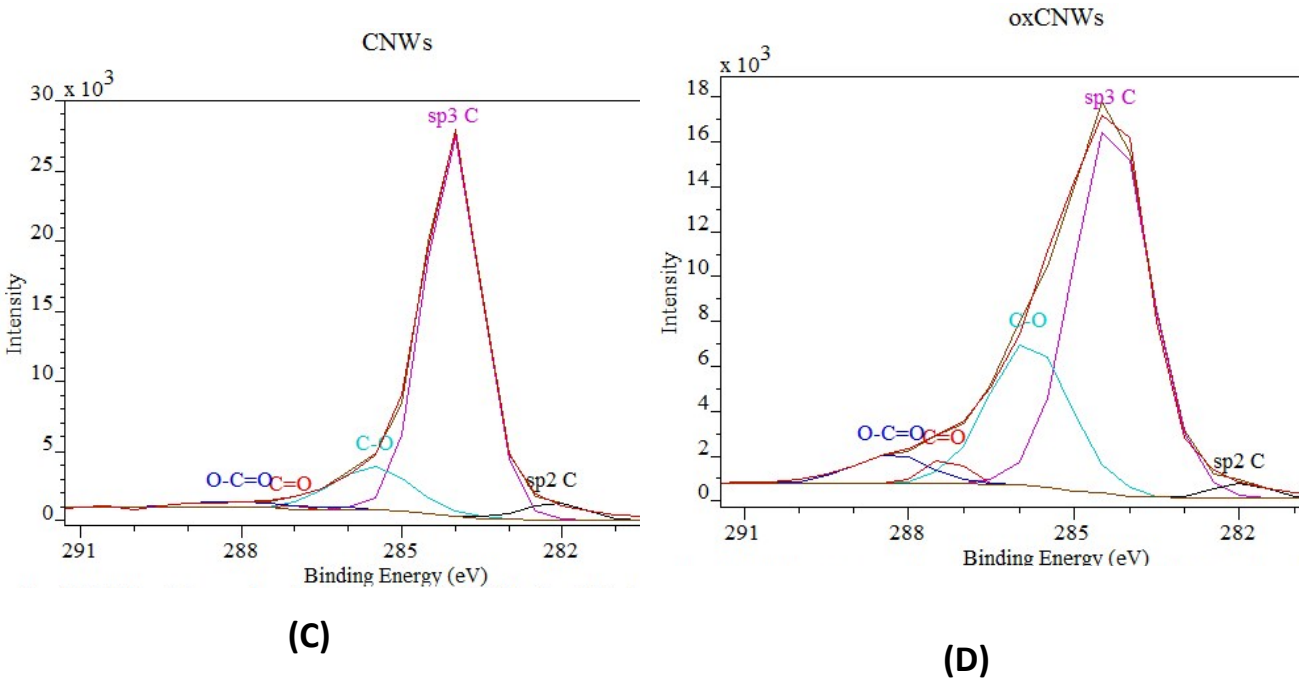

Fig. S4: High resolution of XPS spectra of as-prepared CNWs (red) and after oxidation of CNWs (kaki) for C_{1s} region (A) and O_{1s} region (B). Deconvoluted XPS spectra of C_{1s} for as-prepared CNWs (C) and after oxidation (D).

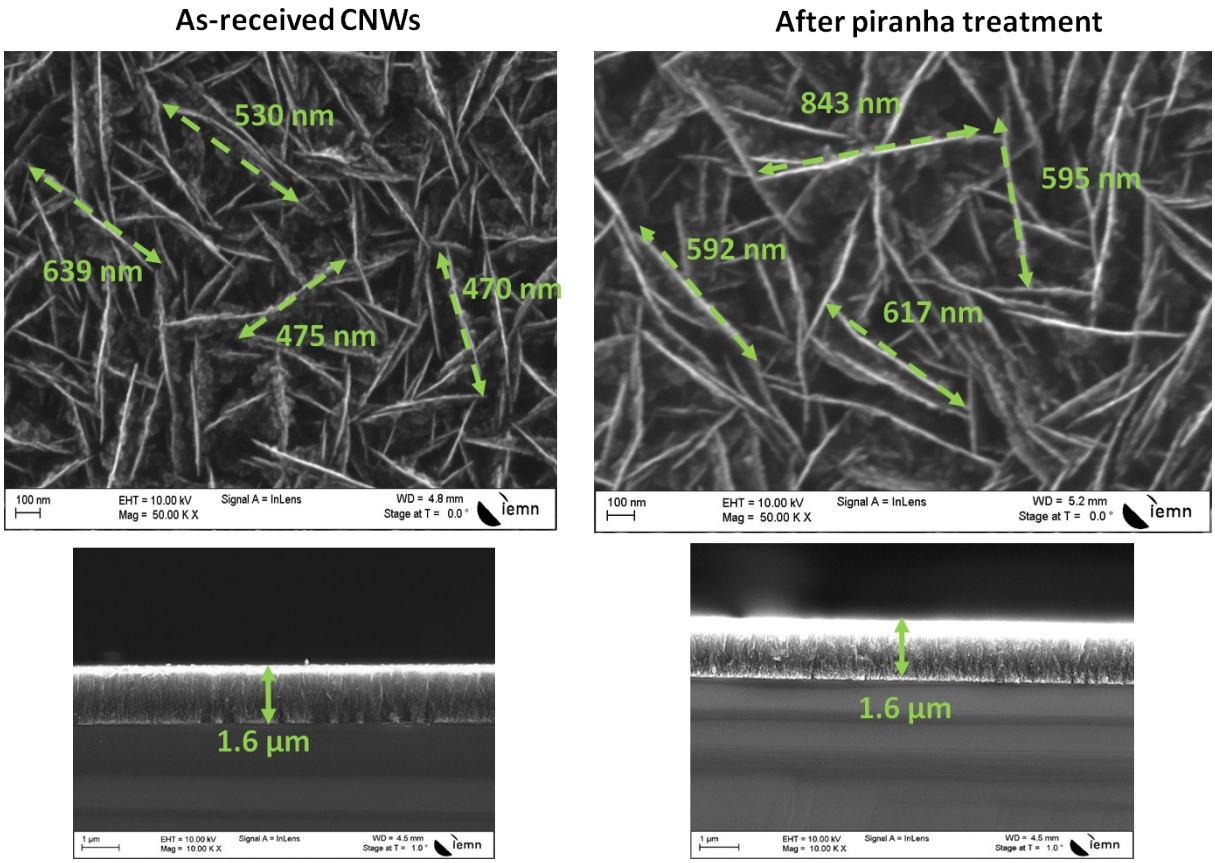

Fig. S5: SEM cross view (A) and top view (B) of CNWs before (left) and after (right) piranha treatment.

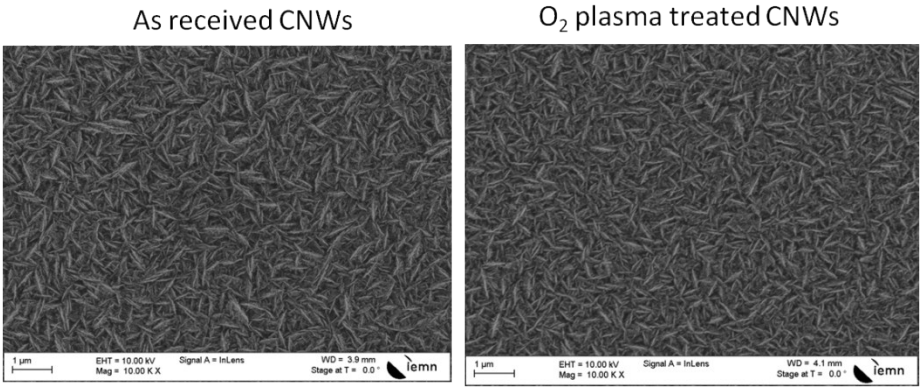

Fig. S6: SEM images of CNWs before and after oxygen plasma treatment.

2.5. Glucose determination in serum

Blood was collected freshly and no coagulant or other chemical was added. After the incubation at room temperature for 30 min, in upright position, the blood was centrifuged during 15 min at 2000 RCF (relative centrifugal force) and the supernatant was pipetted in a new Eppendorf tube. Acetonitrile (ACN)

was added over to precipitate the high abundant proteins (ACN:serum = 3:1, v/v), incubated 10 min at 4°C, and centrifuged again 10 min at 13500 RPM. The supernatant was collected again and the serum was analyzed with UV-Vis and MS or stored at -20°C. For the UV-Vis detection of glucose, 50 µL of serum was diluted in 250 µL of water, and 250 µL of 5% phenol solution was added over. After vortexing the solution, 1.25 mL of sulfuric acid was added rapidly over the mixture, in order to dehydrate glucose and form furan derivatives, that will condensate with the phenol, and form colored compounds.[6] After 10 min at room temperature and 10 min of shaking at 200 RPM, the UV-vis spectra were recorded. The same procedure was followed for the calibration, using glucose dissolved in water. For the MS analysis, 5 µL of serum was dissolved in 25 µL and the solution was drop-casted as described above, without or with spikes of glucose.

3. Results

3.1. Sugars or carbohydrates detection

Xylose (M_w=150.13), one of the smallest saccharides, was dissolved in water in absence and in presence of exogenous Na^+ and drop-casted on CNWs surface (5 nmol), as described in the experimental part. MS spectra were registered and the intensities were compared for different laser powers. Even when Na^+ was not added, the intrinsically presence of Na^+ in the sugar's powder, determined that the main peak was 172.8 m/z corresponding to ($[M_{xylose} + Na]^+$ adduct. The carbon isotopes can also be observed. The added sodium salt, besides increasing the sensitivity, also improved the reproducibility with better RSD values (*e.g.* RSD 16 % for added sodium compared with RSD 80% in absence of added sodium, at laser power of 66%). No response was obtained for smaller power than 62% in absence of added Na^+ sources.

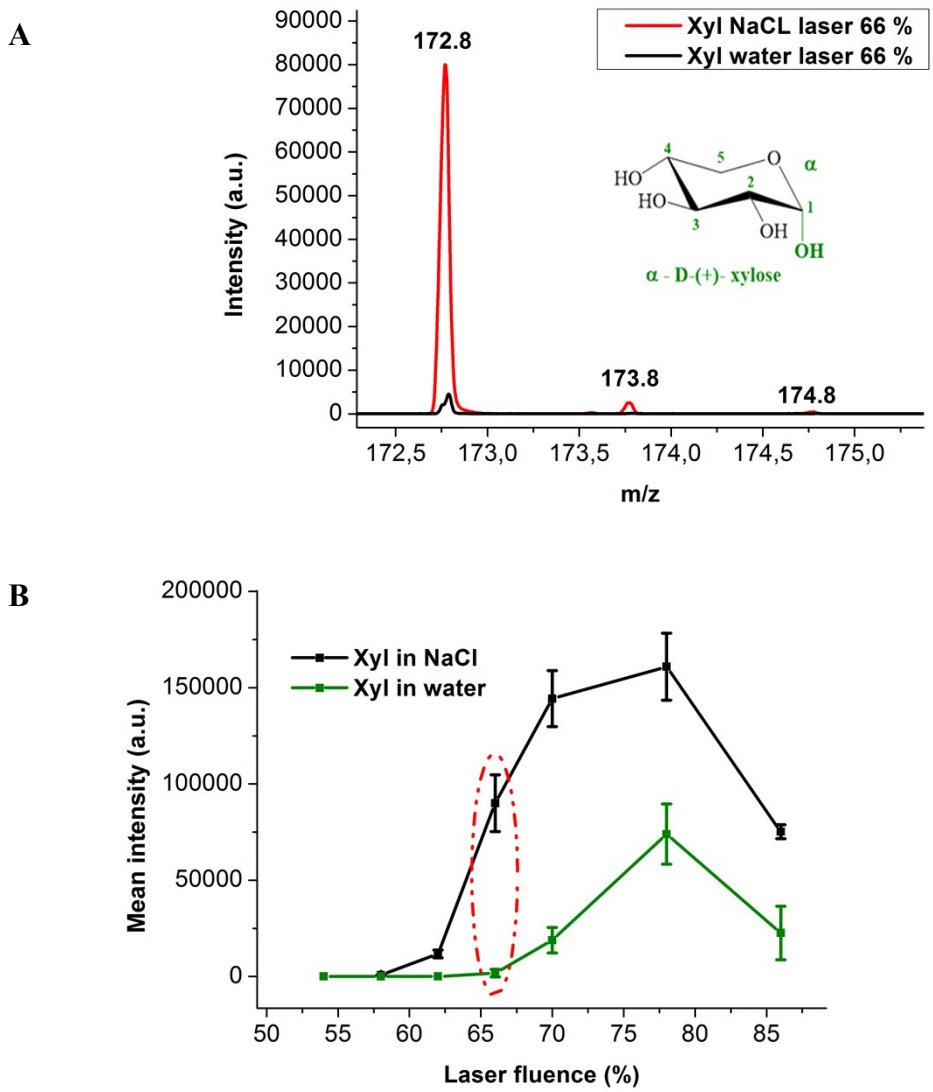

Fig. S7: Mass spectra obtained for Xylose (500 pmol) in NaCl solution (10 mM) (red) and in water (black), at laser power 66 %. Main peak corresponds to $[Xylose+Na]^+$ at 172.8 m/z. The presence of the three isotopes can be observed: ^{12}C(172.8 m/z), ^{13}C(173.8 m/z), while the peak at (174.8 m/z) is the A+2 ion cluster showing the double incorporation of ^{13}C.

(A). The representation of MS signal intensities as a function of laser power for xylose in water (green) and xylose in NaCl (black) (B).

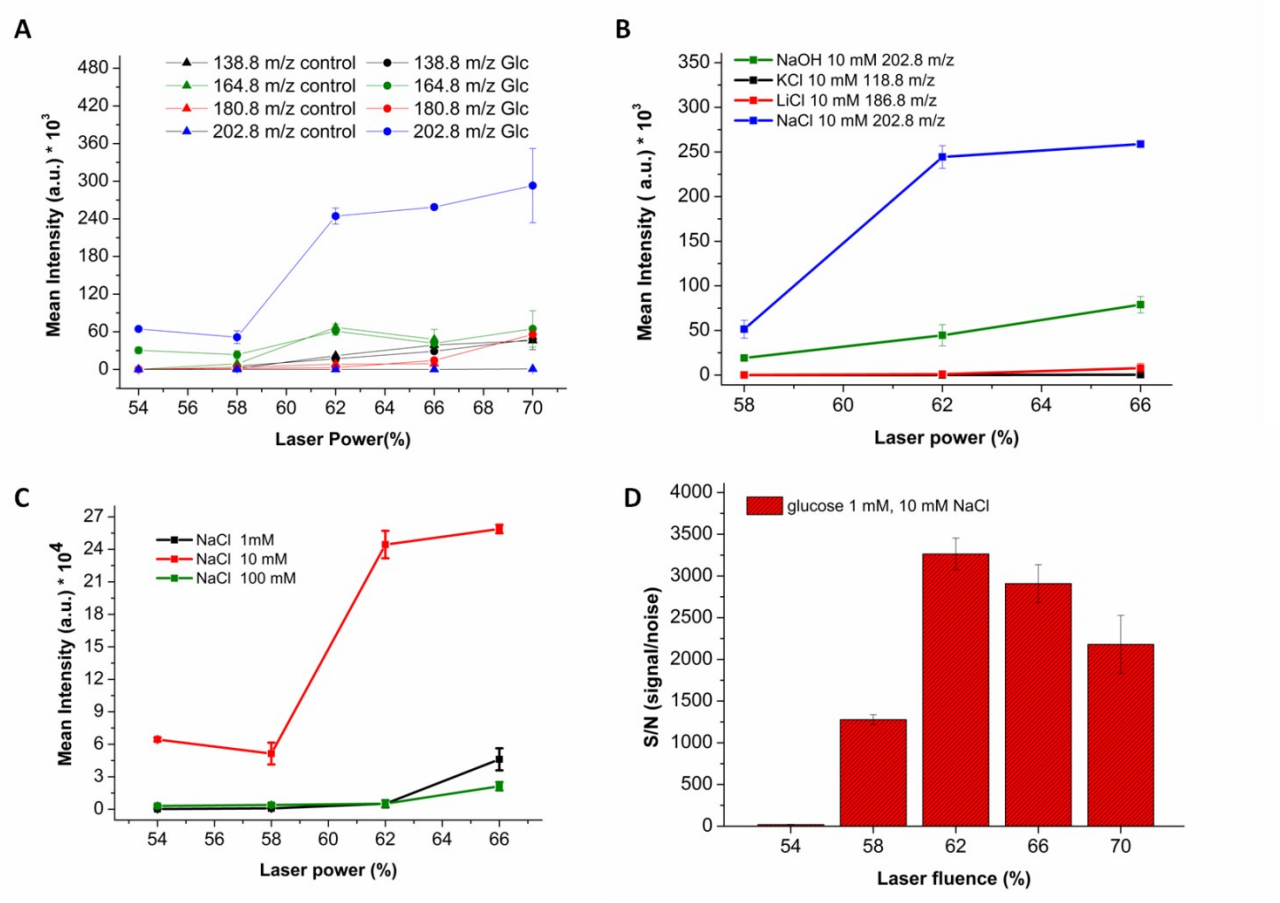

Fig. S8: (A) Comparison of SALDI-MS spectra of the control (triangle) and 500 pmol Glc (circle) at m/z 138.8, 164.8, 180.8 and 202.8; (B) Signal/noise ratios as a function of laser fluence for glucose (0.5 nmol in 10 mM NaCl); (C) Study of the Na^+, K^+ and Li^+ added ions on the glucose (500 nmol) detection; (D) Study of the NaCl concentration on the glucose (500 nmol) detection.

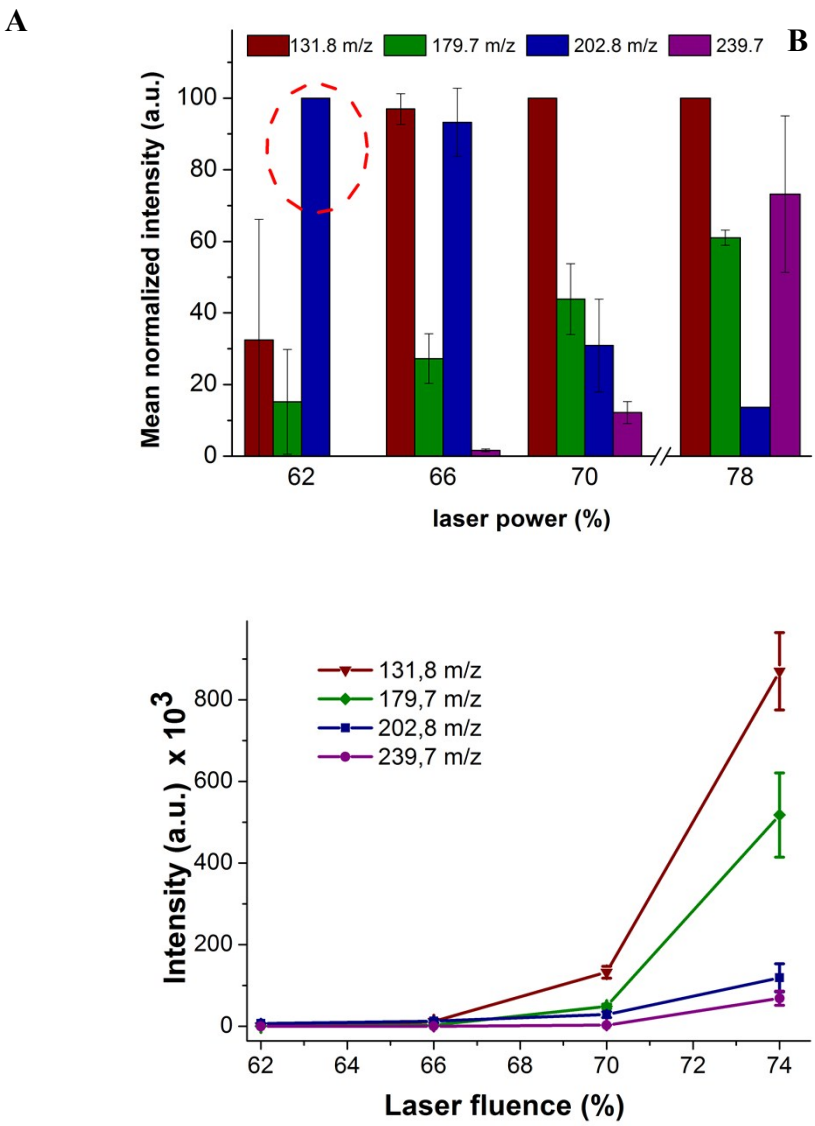

Fig. S9: MS intensities of galactose in water as a function of laser powers for the most four intense peaks.

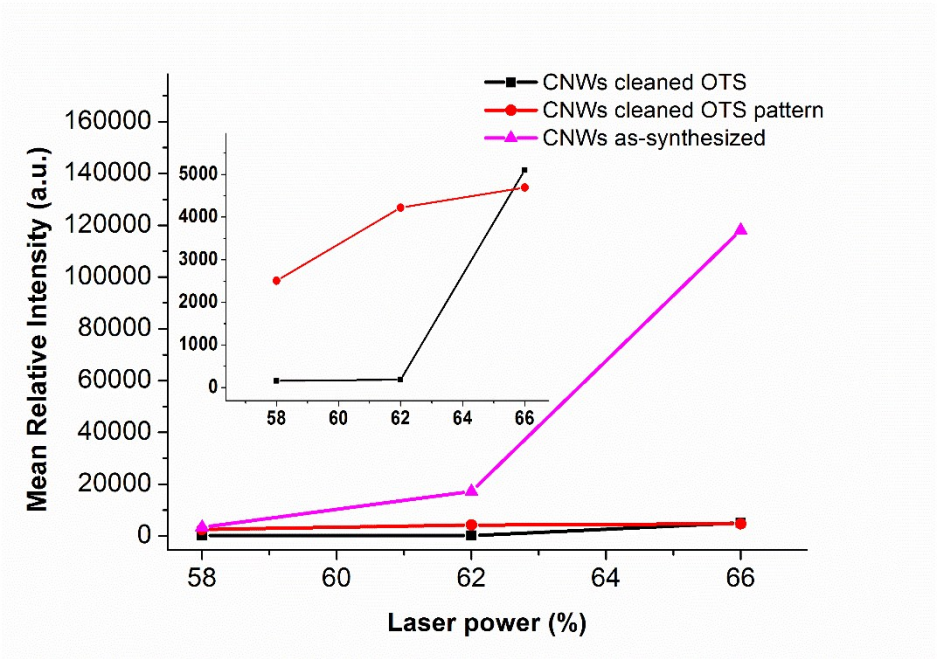

Fig. S10: Comparison of MS signal intensities of 5 nmol glucose at 10 mM in NaCl (10 mM), ($[Glc+Na]^+$ at 202.8 m/z). Glc was either drop casted on CNWs cleaned with piranha and modified with OTS (black) or on CNWs cleaned with piranha, modified with OTS and patterned *via* lithography and oxygen plasma. Inset: zoom for the cleaned oxCNWs surfaces.

Table S3. Comparison between SALDI-MS measurements (n=3 for surface-to-surface and intra-spot measurements and n=6 for inter-spot measurements) done without and with internal standard (250 pmol, D-glucose-2-^{13}C) for glucose (250 pmol, in 10 mM NaCl).

	Without internal standard (203 m/z)		**With internal standard (205/203 m/z ratio)**	
	Mean intensity (±SD)	RSDs (%)	Mean Intensity	RSDs (%)
Inter-spot	55122.67 ± 1468.71	< 9	0.936014 ± 0,018177	< 2
Intra-spot	71273.56 ±14785.08	< 17	0.959888 ± 0,021398	< 2
Inter-surface	56661.93 ± 20861.05	< 36	0.975792 ± 0,016804	< 2.5

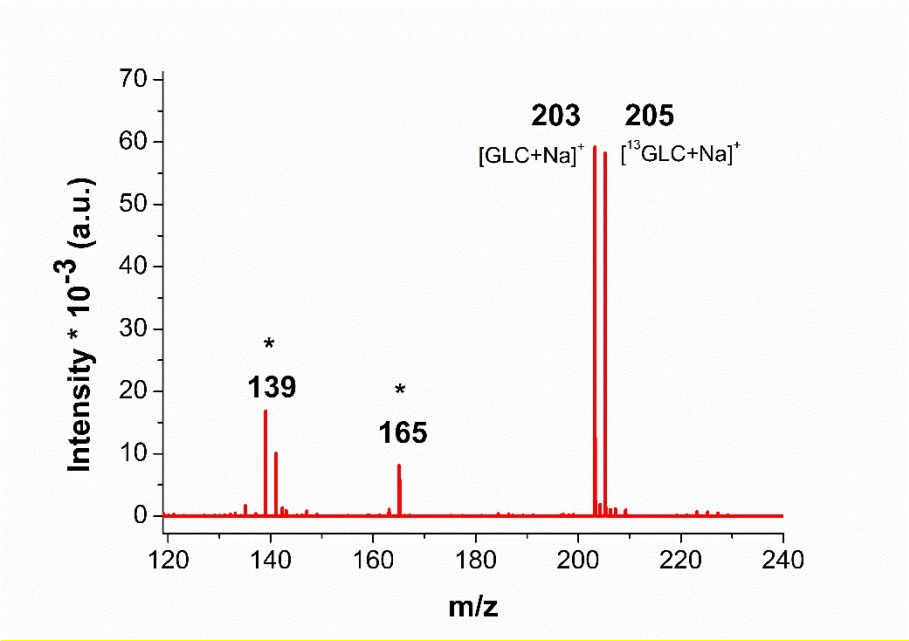

Fig. S11: MS spectrum of glucose (250 pmol) at 203 m/z and ^{13}C glucose (250 pmol) at 205 m/z. The peaks at 139 and 165 m/z correspond to background carbon adducts, as described in the main text.

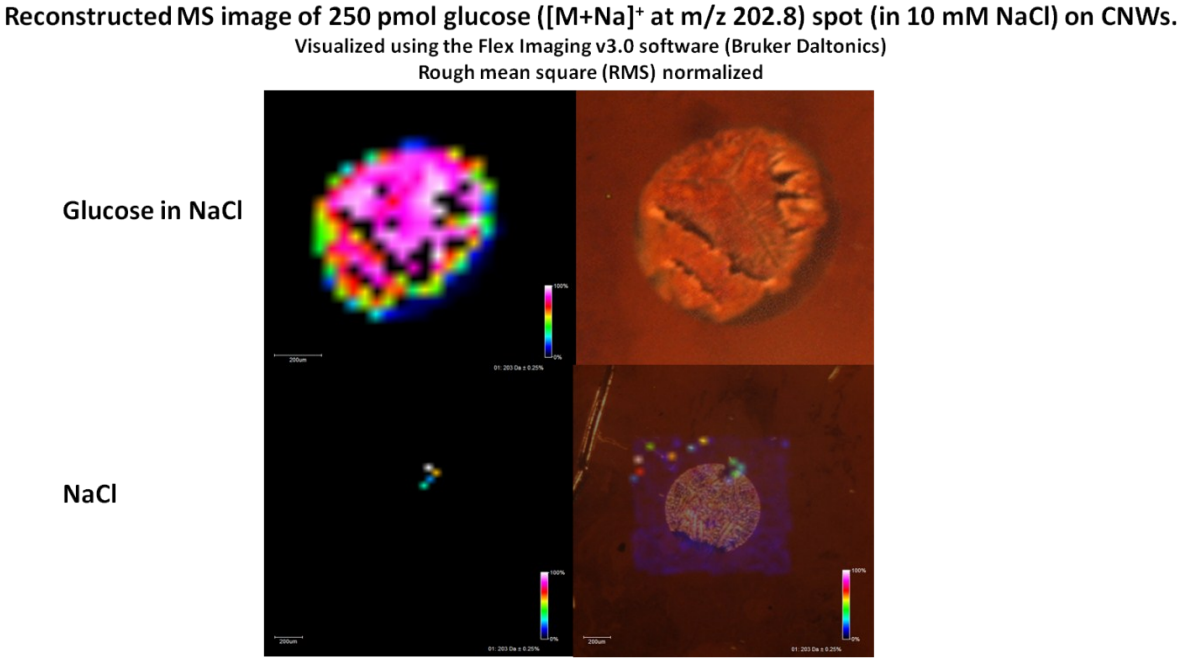

Fig. S12: MS imaging of glucose spot on CNWs. Glucose was detected as sodium adduct [M+Na]+ at m/z 202.8.

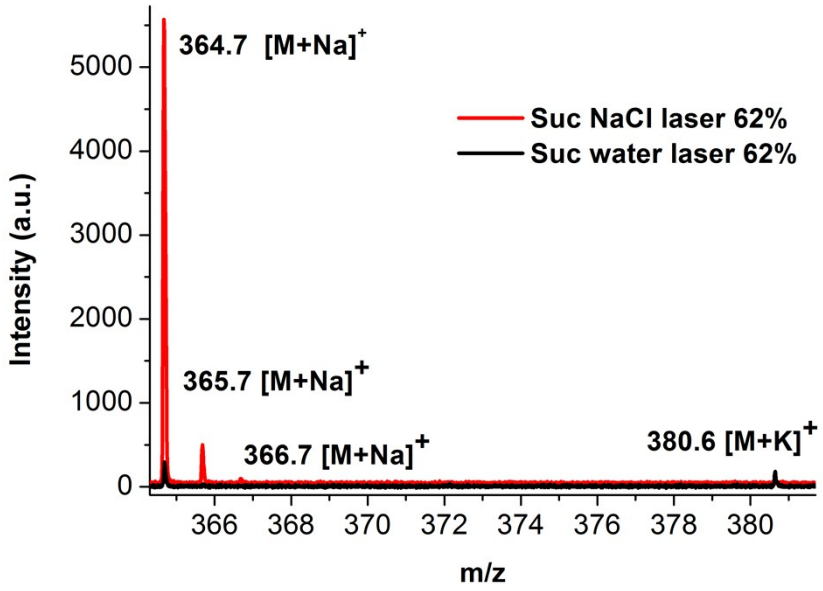

Fig. S13: MS spectra of sucrose (500 pmol in 10 mM NaCl) $[Suc+Na]^+$ and $[Suc+K]^+$ adducts. The presence of the two carbon isotopes can be observed in the presence of NaCl 10mM: ^{12}C(364.7 m/z) and ^{13}C(365.7 m/z). The peak at 366.7 m/z is the A+2 ion of the isotopic cluster showing the double incorporation of ^{13}C.

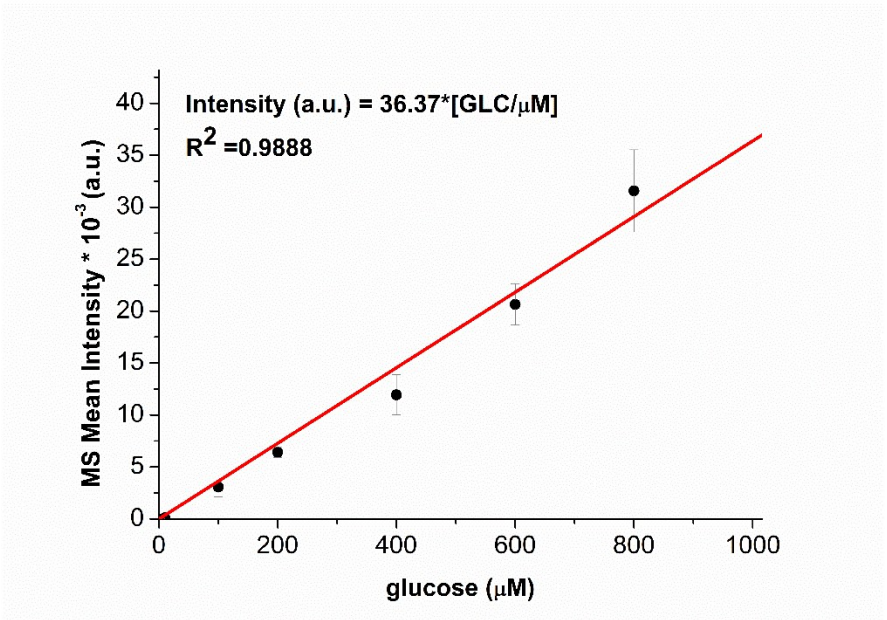

Fig. S14: Calibration curve of glucose, at 202.8 m/z, performed in 10 mM NaCl.

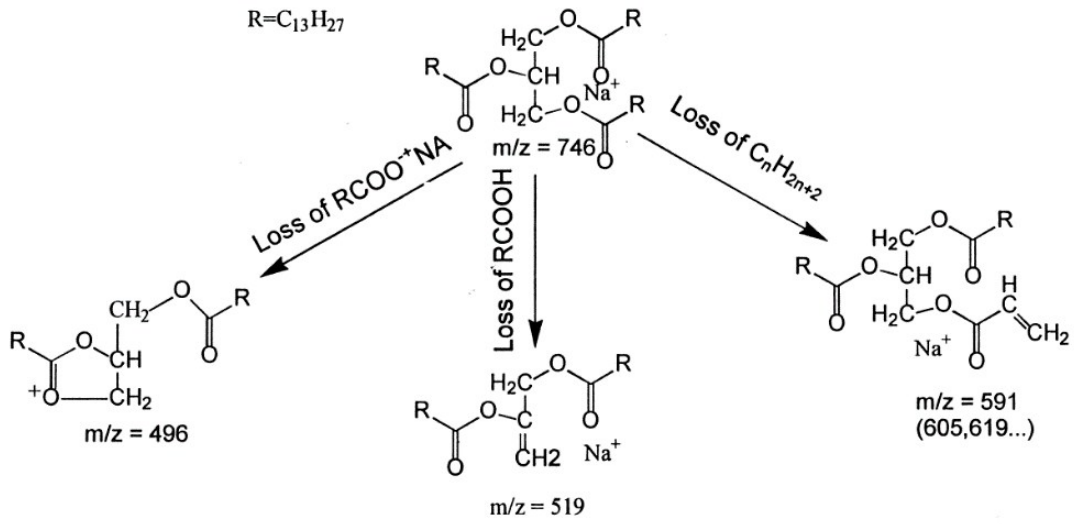

Scheme S3. The major dissociative pathways for TAG's using high energy CID. Reproduced from ref[7] (TAG=triacylglicerides).

Table S4. The variety of molecules studied for detection with the SALDI MS method, in pure solution or in real sample.

Sample n.	**Analyte**	**Peak (m/z)**	**Solvent/Medium**
1.	Glucose	202.8 $[M+Na]^+$ 218.8 $[M+K]^+$	Water NaCl 10 mM Blood serum Coca Cola
2.	Gluconic acid	219 $[M+Na]^+$ 241 m/z $[M+2Na-H]^+$	Water NaCl 10 mM Blood serum
3.	Fructose	202.8 $[M+Na]^+$	Water NaCl 10 mM Coca Cola
4.	Xylose	172.8 $[M+Na]^+$	Water NaCl 10 mM
5.	Sucrose	364.7 $[M+Na]^+$ 202.8 $[M-+Na]^+$	Water NaCl 10 mM Coca Cola
6.	Galactose	202.8 $[M+Na]^+$	Water NaCl 10 mM
7.	Paracetamol	152 $[M+H]^+$	water urine

8.	3 nitro-acetaminophen	197 $[M+H]^+$	urine
9.	Dopamine	154 $[M+H]^+$ 136 $[M-NH_3]^+$ 176 $[M+Na]^+$ 192 $[M+K]^+$	water
10.	Melamine	127 $[M+H]^+$ 149 $[M-NH_3]$	water
11.	Uric Acid	168.9 $[M+H]^+$ 142.8 m/z $[M-?]^+$	water
12.	Glycerol	114.8 $[M+Na]^+$	water
13.	Caffeine	194.9 $[M+H]^+$	water
14.	Lecithin	791 $[M+Na]^+$	Water/EtOH Food supplement
15.	Oleic acid	327.7 $[M-H+2Na]^+$	Water/EtOH Food supplement
16.	Stearic acid	329.7 $[M-H+2Na]^+$	Water/EtOH Food supplement
17.	Palmitic Acid	301.7 $[M-H+2Na]^+$	Water/EtOH Food supplement
18.	Creatinine	114 $[M+H]^+$, 136 $[M+Na]^+$	Urine
19.	Insulin (bovine)	5734 $[M+Na]^+$	Ammonium citrate dibasic
20.	Cytochrome C	-	Ammonium citrate dibasic
21.	Bovine Serum Albumin	-	Ammonium citrate dibasic
22.	Apomyoglobin (horse)	-	Ammonium citrate dibasic
23.	Thioredoxin (E. coli)	-	Ammonium citrate dibasic

24.	Dextran	-	Ammonium citrate dibasic
25.	Cyano- benzylpyridinium	195 $[M+H]^+$, 116 $[M\text{-pyridine}+H]^+$,	water

3.2. References

1. R. Bogdanowicz, M. Sobaszek, J. Ryl, M. Gnyba, M. Ficek, Ł. Gołuński, W. J. Bock, M. Śmietana and K. Darowicki, *Diamond and Related Materials*, 2015, **55**, 52-63.
2. R. Bogdanowicz, *Metrology and Measurement Systems*, 2014, **21**, 685-698.
3. Y. Coffinier, S. Szunerits, H. Drobecq, O. Melnyk and R. Boukherroub, *Nanoscale*, 2012, **4**, 231-238.
4. G. Piret, H. Drobecq, Y. Coffinier, O. Melnyk and R. Boukherroub, *Langmuir*, 2009, **26**, 1354-1361.
5. P. M. Flanigan IV, F. Shi, J. J. Perez, S. Karki, C. Pfeiffer, C. Schafmeister and R. J. Levis, *Journal of the American Society for Mass Spectrometry*, 2014, **25**, 1572-1582.
6. J. N. BeMiller, in *Food analysis*, Springer, 2010, pp. 147-177.
7. G. R. Asbury, K. Al-Saad, W. F. Siems, R. M. Hannan and H. H. Hill Jr, *Journal of the American Society for Mass Spectrometry*, 1999, **10**, 983-991.